Supplementary Information for

Lewis acidity driven fluorochromism in a lanthanide MOF for highly selective Zr(IV) detection

Tianxing Wang,[a,‡] Xinhui Dong,[a,‡] Yishan Hou,[a,‡] Shuhan Liu,[a,‡] Yue Yan,[a] Xinyuan Mao,[a] Yongxin Li,[b] Yunyi Cui,[a,*] and Jian Lin[a,*]

a. School of Nuclear Science and Technology, Xi'an Jiaotong University, Xi'an 710049, PR China.

E-mail: cuiyunyi@stu.xjtu.edu.cn, jianlin@xjtu.edu.cn

b. Division of Chemistry and Biological Chemistry, School of Physical and Mathematical Sciences, Nanyang Technological University, 637371, Singapore

Experimental Section

Materials

Caution! Uranyl nitrate ($UO_2(NO_3)_2·6H_2O$) is radioactive and chemically toxic. All uranium compounds utilized in this study were handled in a certified laboratory designed specifically for the manipulation of actinide elements, ensuring compliance with established safety protocols for working with radioactive materials.

$UO_2(NO_3)_2·6H_2O$ (99%) were purchased from International Bio-Analytical Industries. N,N-dimethylformamide (DMF) (99.5%), $RbNO_3$ (99%), $Fe(NO_3)_3·9H_2O$ (99.99%), $Cd(NO_3)_2·4H_2O$ (99%), $Y(NO_3)_3·6H_2O$ (99.5%), $Ce(NO_3)_3·6H_2O$ (99.99%), $Eu(NO_3)_3·6H_2O$ (99.99%), $Gd(NO_3)_3·6H_2O$ (99.99%), $NbCl_5$ (99%), K_2CrO_4 (99.5%), Na_2MoO_4 (99%), and $NaReO_4$ (99.95%) were purchased from Shanghai Macklin Biochemical Technology Co., Ltd. 2-fluorobenzoic acid (2-FBA) (≥ 98%), NaCl (99.5%), $MnCl_2·4H_2O$ (99.99%), and KI (99%) were purchased from Shanghai Aladdin Biochemical Technology Co., Ltd. Nitric acid (HNO_3) (≥ 99.7%), ethanol (≥ 99.7%), $AgNO_3$ (≥ 99.5%), $Ni(NO_3)_2·6H_2O$ (≥ 99.5%), $Ba(NO_3)_2$ (≥ 99.5%), $Sr(NO_3)_2$ (≥ 99.5%), $CsNO_3$ (≥ 99.5%), and $La(NO_3)_3$ (≥ 99.5%) were purchased from Sinopharm Chemical Reagent Co., Ltd. $CoCl_2$ (98%), Na_2SeO_3 (99%), and $NaIO_3$ (99%) were Shanghai Titan Scientific Co., Ltd. All chemicals and reagents were analytically pure and used without further purification.

Synthesis of Eu-BPTC

Two different synthetic routes were employed to optimize crystal size and reaction yield. Eu-BPTC was synthesized under solvothermal conditions employing 2-fluorobenzoic acid (2-FBA) as a modulator. For the growth of single crystals, $Eu(NO_3)_3·6H_2O$ (4.46 mg, 0.01 mmol), H_4BPTC (1.65 mg, 0.005 mmol), and 2-FBA (22.42 mg, 0.16 mmol) were dissolved in a mixture of DMF (1800 μL), deionized water (200 μL), and concentrated HNO_3 (100 μL) within a 7 mL glass vial. The sealed vessel was heated at 120 °C for 72 h and subsequently cooled to room temperature.

For the bulk preparation, an acid-free strategy (without the addition of HNO_3) was adopted under otherwise identical conditions, which significantly improved the product yield (51.5%). The resulting microcrystals was harvested, washed with DMF and ethanol, and air-dried. The experimental PXRD pattern of the bulk Eu-BPTC microcrystal powder is in good agreement with the simulated one derived from the single-crystal data, confirming their phase purity.

General Characterization

SCXRD data was collected at 150 K on a Bruker D8-Venture diffractometer equipped with an IμS 3.0 microfocus source (Mo–Kα radiation, λ= 0.71073Å) and a CMOS detector. The collection and reduction of single crystal diffraction data were completed in *APEX4* program. Analysis of the unit cell parameters and space group confirmed that Eu-BPTC is isostructural to the previously reported Y-BPTC (CCDC number: 1843058) and Ce-BPTC (CCDC number: 2205374). The simulated PXRD pattern of Eu-BPTC was consistent with that of the Y-BPTC/Ce-BPTC crystals, and the phase purity of the bulk powder was further validated by the agreement between the experimental and simulated patterns.

PXRD patterns were recorded on a Bruker D8 Advance diffractometer (40 kV, 40 mA, Cu Kα radiation, λ = 1.54060 Å) scanning from 5° to 35° (2θ) with a step size of 0.02°. The simulated PXRD pattern of Eu-BPTC was derived from the single-crystal data using Materials Studio program. Photoluminescence properties, including emission spectra, lifetimes, and quantum yields, were determined using an Edinburgh FLS980 fluorescence spectrometer at room temperature. FTIR spectra were acquired on a PerkinElmer Spectrum 3 spectrometer in the range of 4000 – 600 cm^{-1}.

UV-Vis absorption spectra were collected in the wavelength range of 200 – 800 nm using a Shimadzu UV-2700i spectrophotometer. TGA was performed on a METTLER TOLEDO TGA/DSC 3+ instrument from 35 °C to 800 °C at a heating rate of 10 °C min^{-1} under a continuous N_2 atmosphere. The morphology and elemental distribution of Eu-BPTC before and after soaking in Zr(IV) solution were characterized using a GeminiSEM 500 scanning electron microscope (SEM) equipped with an energy-dispersive X-ray spectroscopy (EDS) detector. Solutions of Eu-BPTC, H4BPTC, and Zr(IV)-soaked Eu-BPTC powder (5 mg) were prepared by digestion in a mixture of D_2SO_4 (150 μL) and DMSO-d_6 (450 μL). ^1H NMR spectra were collected at 298 K on a Bruker Avance NEO 400 MHz Spectrometer and processed using MestReNova software. Chemical shifts were referenced to the residual DMSO-d_6 solvent signal.

Fluorochromic Detection of Zr(IV)

To ensure uniform dispersion and maximize analyte interaction, Eu-BPTC crystals were ground into a fine microcrystalline powder with an average particle size of approximately 0.65 μm. In each experiment, a homogenous suspension (solid–liquid ratio of 1mg mL^{-1}) was prepared by dispersing 2.5 mg of the powder in 2.5 mL of deionized water under magnetic stirring for 1 hour. For sensing assays, Eu-BPTC suspension was transferred to a quartz cuvette and titrated stepwise with aqueous Zr(IV) (20 mM) to achieve concentrations ranging from 0 to 5.7 mM (pH 2.07). To ensure reproducibility and mitigate instrumental deviations, all fluorescence spectra were collected three times.

To strictly account for the dilution effect caused by the stepwise addition of the Zr(IV) stock solution during the titration process, the observed fluorescence intensities were mathematically corrected.

$$I' = I \times \frac{V_0 + V_a}{V_0}$$

where I' is the corrected fluorescence intensity. I is the experimentally observed fluorescence intensity. V_0 is the initial volume of the suspension (2.5 mL). V_a is the volume of the added Zr(IV) solution at each titration point.

The limit of detection (LOD) as calculated by the equation:

$$LOD=3\sigma/k$$

where σ is the standard deviation of the fluorescence intensity of the Eu-BPTC suspension prior to the addition of Zr(IV), and k represents the absolute value of slope obtained from the linear fit of luminescence intensity at 612 nm versus Zr(IV) concentration (0 – 1.13 mM).

Detection Selectivity Study

In each experiment, 3 mg of Eu-NDC powder was dispersed in 3 mL of a Zr(IV) (pH 2.15) and competing ion solution, respectively. The competing ions tested included Na(I), Rb(I), Ag(I), Cs(I), Mn(II), Co(II), Ni(II), Cd(II), Sr(II), Ba(II), Fe(III), Y(III), La(III), Ce(III), Eu(III), Gd(III), Nb(V), and U(VI), all introduced via their respective chloride or nitrate salts. Additionally, the influence of anions, including NO_3^-, CrO_4^{2-}, SeO_3^{2-}, MoO_4^{2-}, ReO_4^-, I^-, and IO_3^-, was evaluated using their sodium or potassium salts. After the suspensions were equilibrated for 2 hours, all fluorescence spectra were collected three times to ensure reproducibility and mitigate instrumental deviations.

Supplementary Figures

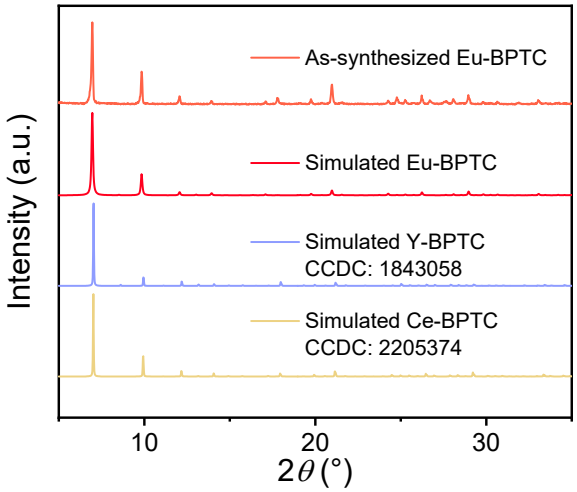

Fig. S1 PXRD patterns of as-synthesized Eu-BPTC, simulated Eu-BPTC, simulated Y-BPTC (CCDC: 1843058), and simulated Ce-BPTC (CCDC: 2205374).

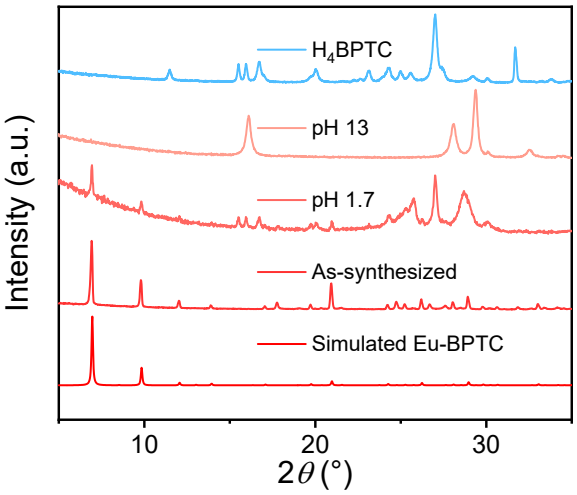

Fig. S2 PXRD patterns of Eu-BPTC before and after immersion at pH 1.7 and pH 13 for 24 hours, compared with the simulated patterns of H_4BPTC and Eu-BPTC.

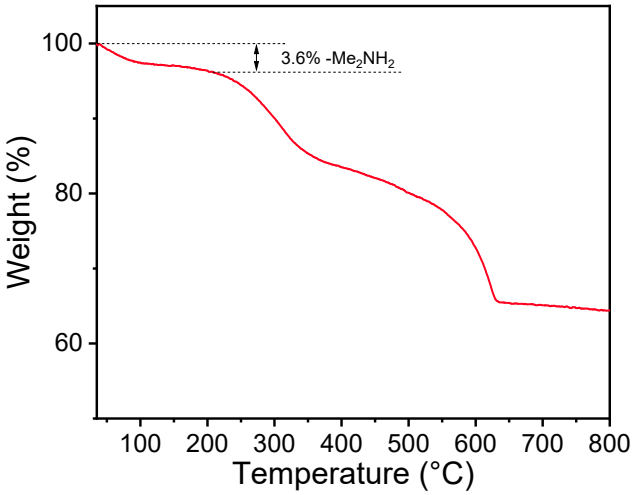

Fig. S3 Thermogravimetric analysis (TGA) of Eu-BPTC.

The thermogravimetric analysis (TGA) profile showed an initial weight loss in the range of 35–200 °C, which is attributed to the removal of $[Me_2NH_2]^+$ counterions. Upon further heating, the framework undergoes progressive thermal decomposition and is fully decomposed by approximately 630 °C.

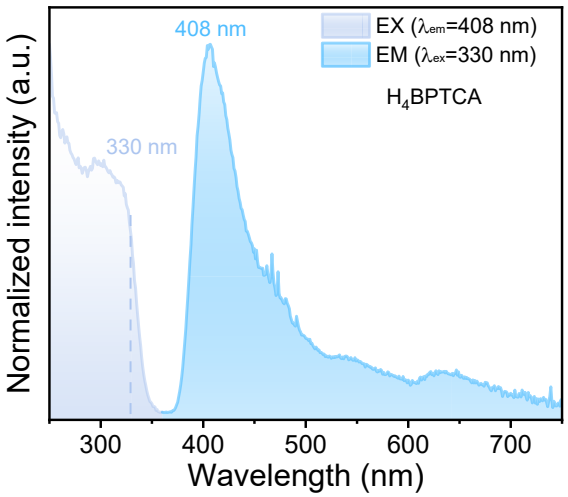

Fig. S4 Excitation and emission spectra of H_4BPTC.

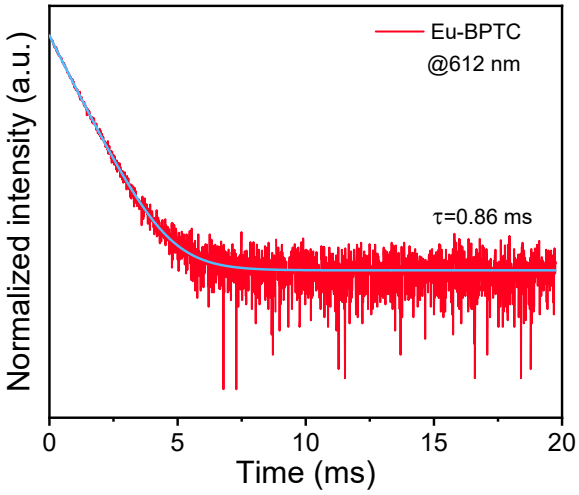

Fig. S5 Time-resolved photoluminescence decay of Eu-BPTC at 612 nm.

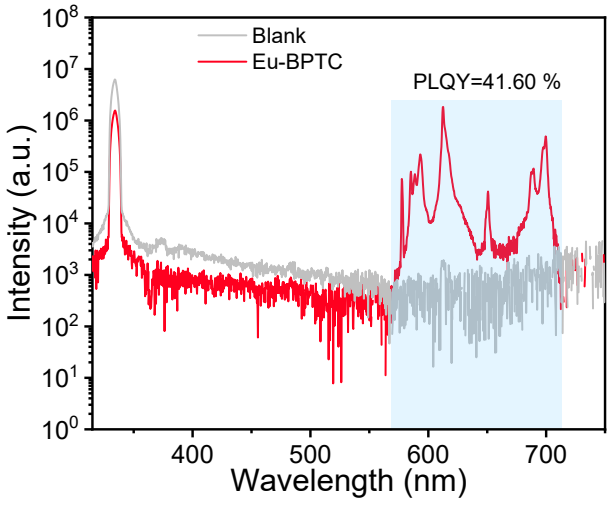

Fig. S6 Photoluminescence quantum yield (PLQY) of Eu-BPTC (λ_{ex} = 330 nm).

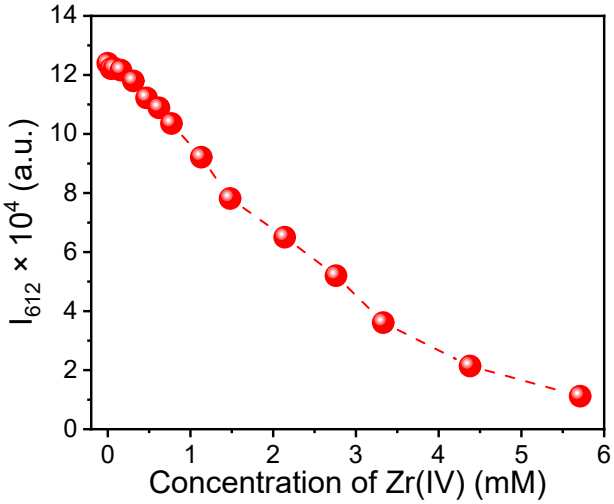

Fig. S7 Correlation between luminescence intensity at 612 nm (I_{612}) of Eu-BPTC and Zr(IV) concentration.

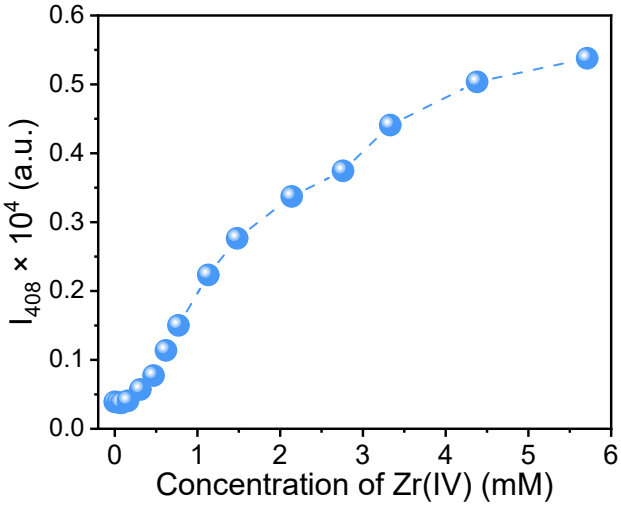

Fig. S8 Correlation between luminescence intensity at 408 nm (I_{408}) of Eu-BPTC and Zr(IV) concentration.

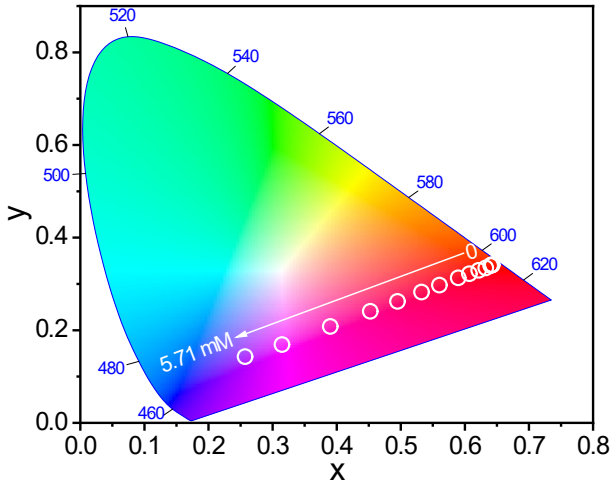

Fig. S9 Commission Internationale de l'Éclairage (CIE) chromaticity coordinates of the Eu-BPTC suspension as a function of Zr(IV) concentration.

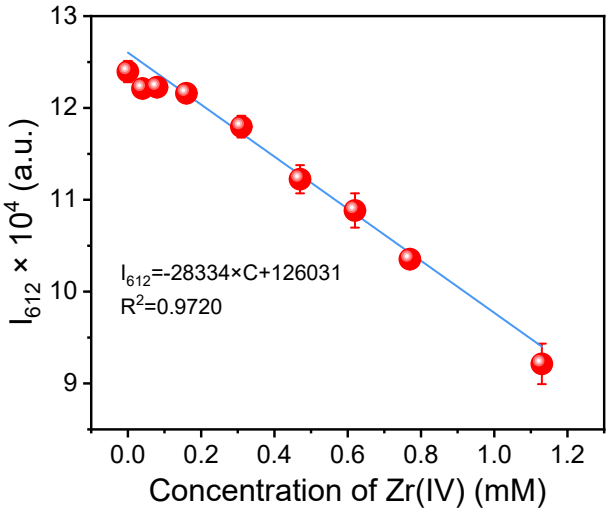

Fig. S10 Linear fit of I_{612} as a function of Zr(IV) concentration ranging from 0 to 1.13 mM.

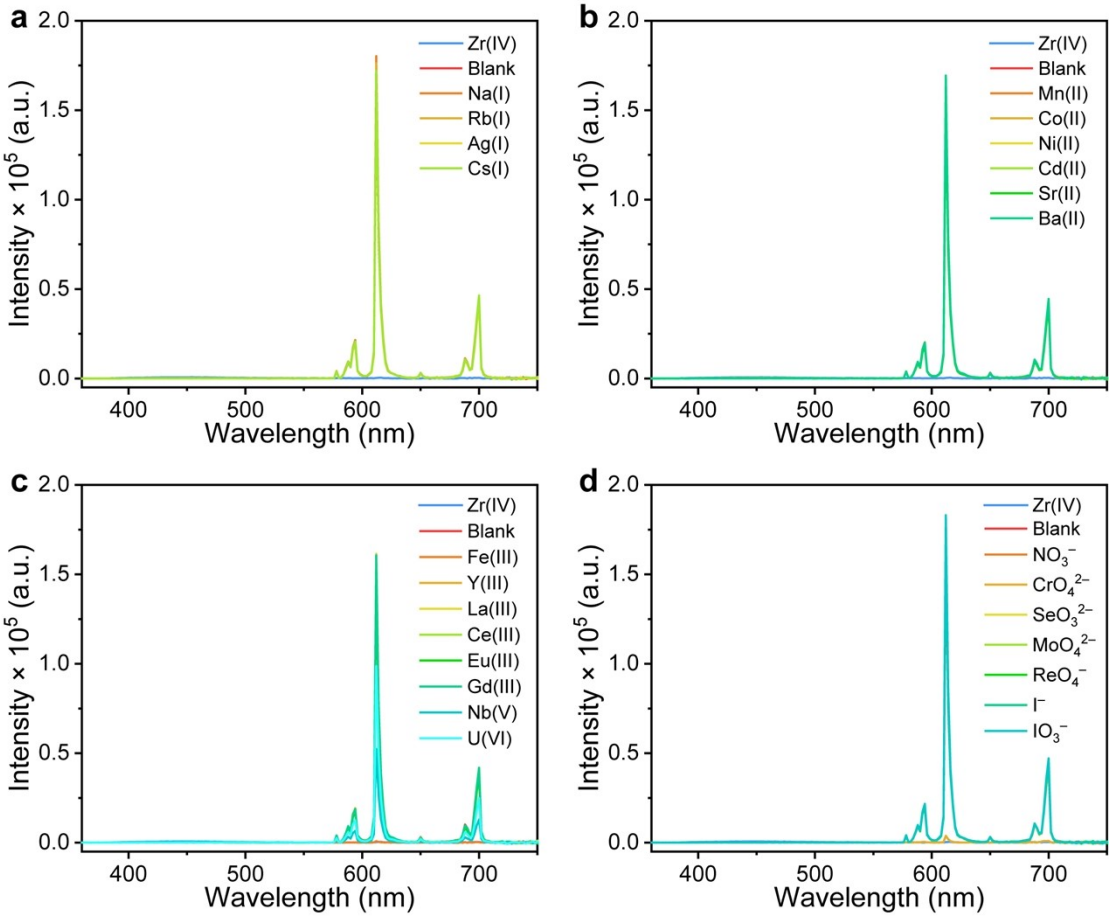

Fig. S11 Photoluminescence spectra of Eu-BPTC in 7 mM aqueous solutions of Zr(IV) and (a) Na(I), Rb(I), Ag(I), and Cs(I); (b) Mn(II), Co(II), Ni(II), Cd(II), Sr(II), and Ba(II); (c) Fe(III), Y(III), La(III), Ce(III), Eu(III), Gd(III), Nb(V), and U(VI); and (d) anions including NO_3^-, CrO_4^{2-}, SeO_3^{2-}, MoO_4^{2-}, ReO_4^-, I^-, and IO_3^-.

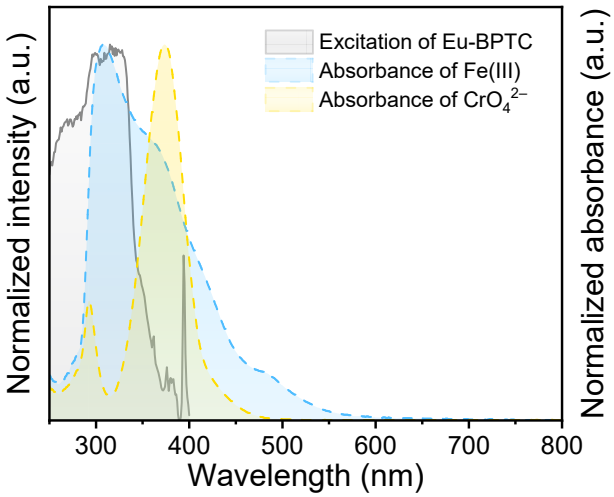

Fig. S12 The UV-Vis absorption spectra of Fe(III) and CrO_4^{2-} solutions compared with the excitation spectrum of Eu-BPTC.

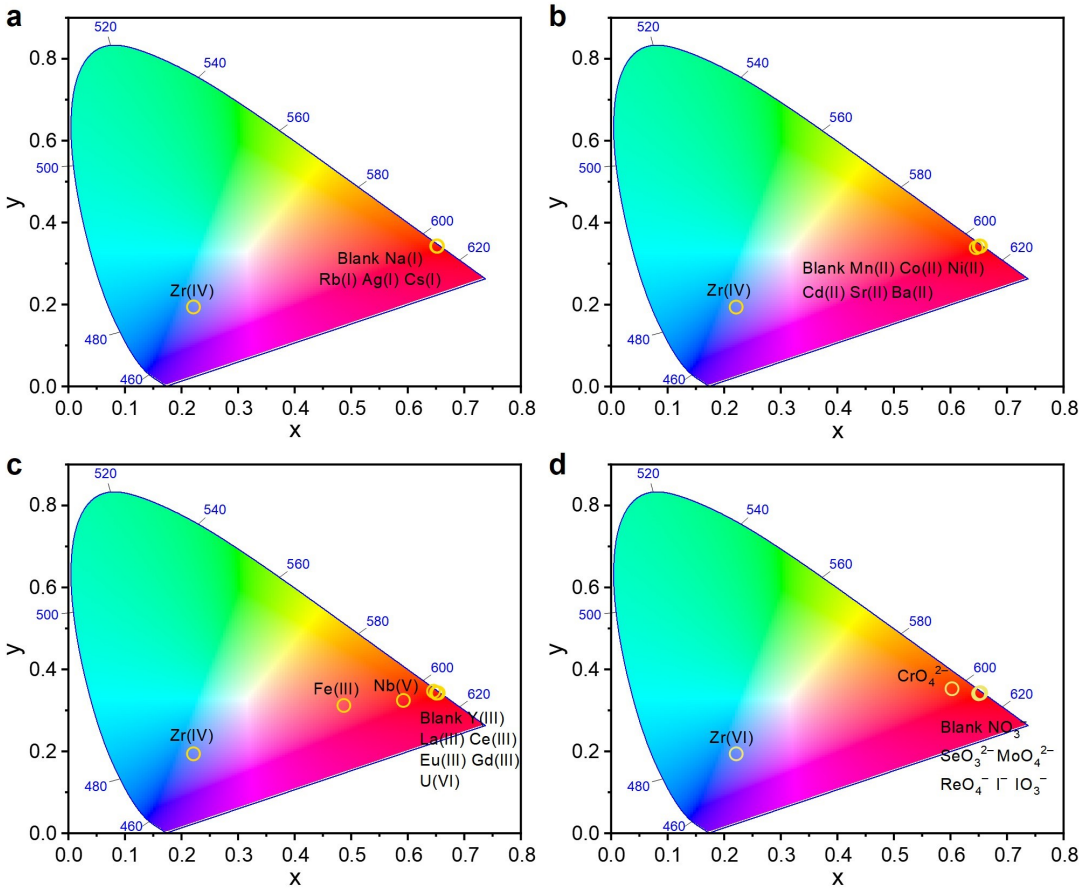

Fig. S13 CIE chromaticity coordinates of the Eu-BPTC suspensions treated with 7 mM Zr(IV) and various competing ions solution: (a) Na(I), Rb(I), Ag(I), and Cs(I); (b) Mn(II), Co(II), Ni(II), Cd(II), Sr(II), and Ba(II); (c) Fe(III), Y(III), La(III), Ce(III), Eu(III), Gd(III), Nb(V), and U(VI); and (d) anions including NO_3^-, CrO_4^{2-}, SeO_3^{2-}, MoO_4^{2-}, ReO_4^-, I^-, and IO_3^-.

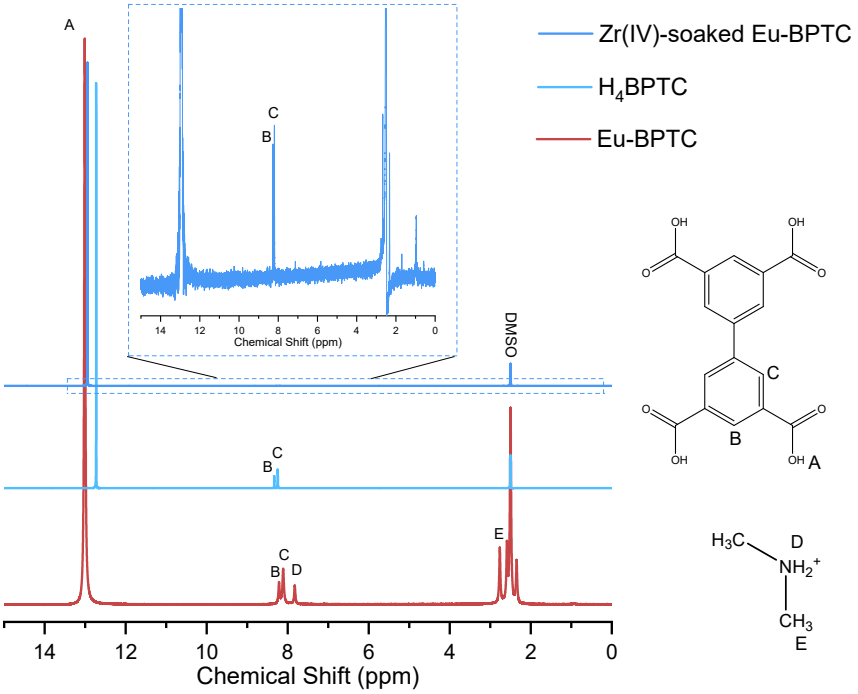

Fig. S14 ^{1}H NMR spectra (400 MHz, DMSO-d_6 with D_2SO_4) of Eu-BPTC, H_4BPTC, and Zr(IV)-soaked Eu-BPTC. **Inset:** Zoomed-in view of the Zr(IV)-soaked Eu-BPTC spectrum.

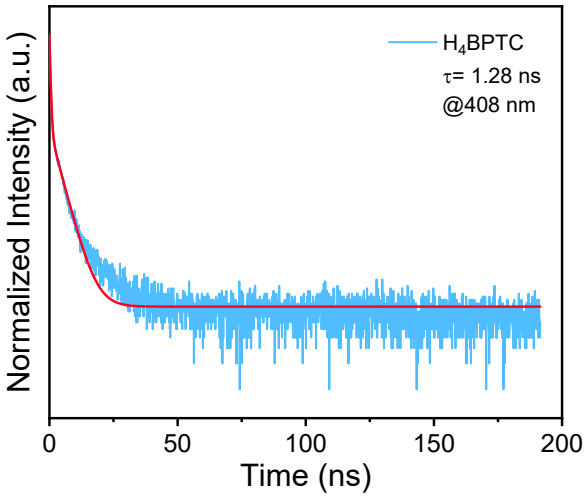

Fig. S15 Time-resolved photoluminescence decay of H_4BPTC at 408 nm.

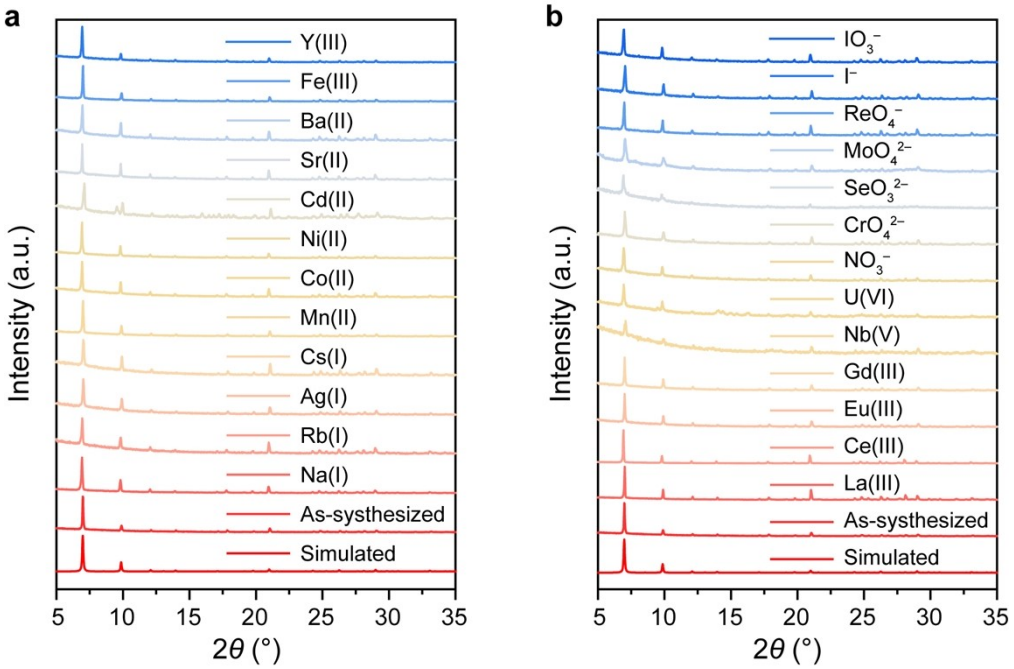

Fig. S16 PXRD patterns of Eu-BPTC before and after exposure to Zr(IV) and various competing ions solution: (a) Na(I), Rb(I), Ag(I), and Cs(I); (b) Mn(II), Co(II), Ni(II), Cd(II), Sr(II), Ba(II), Fe(III), and Y(III); (b) La(III), Ce(III), Eu(III), Gd(III), Nb(V), U(VI), NO_3^-, CrO_4^{2-}, SeO_3^{2-}, MoO_4^{2-}, ReO_4^-, I^-, and IO_3^-.

Supplementary Table

Table S1 Comparison of unit cell parameters for Eu-BPTC and its isostructural analogues.

Compound	**Eu-BPTC**	**Y-BPTC**	**Ce-BPTC**
Ref.	This work	CCDC: 1843058	CCDC: 2205374
Formula	$C_{48}H_{36}O_{30}F_8Eu_6$	$C_{55}H_{60}N_3O_{38.5}Y_6$	$C_{48}H_{22}O_{32}Ce_6$
Formula weight	2120.37	1912.52	1951.37
Space group	$Im\bar{3}$	$Im\bar{3}$	$Im\bar{3}$
a (Å)	25.3283(8)	25.1402(7)	25.1845(7)
b (Å)	25.3283(8)	25.1402(7)	25.1845(7)
c (Å)	25.3283(8)	25.1402(7)	25.1845(7)
α (deg)	90	90	90
β (deg)	90	90	90
γ (deg)	90	90	90
V (Å^3)	16248.7(15)	15889(1)	15973.5(14)